Published in final edited form as:
Exp Neurol. 2012 January ; 233(1): 243–252. doi:10.1016/j.expneurol.2011.10.009.

Neuronal activity and axonal sprouting differentially regulate CNTF and CNTF receptor complex in the rat supraoptic nucleus

Jason M. Askvig[a], **Laura J. Leiphon**[a], and **John A. Watt**[a]

Jason M. Askvig: jason.askvig@my.und.edu; Laura J. Leiphon: laura.leiphon@med.und.edu; John A. Watt: john.watt@med.und.edu

[a]Department of Anatomy & Cell Biology, University of North Dakota School of Medicine and Health Sciences, Grand Forks, ND 58203, USA

Abstract

We demonstrated previously that the hypothalamic supraoptic nucleus (SON) undergoes a robust axonal sprouting response following unilateral transection of the hypothalamo-neurohypophysial tract. Concomitant with this response is an increase in ciliary neurotrophic factor (CNTF) and CNTF receptor alpha (CNTFRα) expression in the contralateral non-uninjured SON from which the axonal outgrowth occurs. While these findings suggest that CNTF may act as a growth factor in support of neuronal plasticity in the SON, it remained to be determined if the observed increase in neurotrophin expression was related to the sprouting response per se or more generally to the increased neurosecretory activity associated with the post-lesion response. Therefore we used immunocytochemistry and Western blot analysis to examine the expression of CNTF and the components of the CNTF receptor complex in sprouting versus osmotically-stimulated SON. Western blot analysis revealed a significant increase in CNTF, CNTFRα, and gp130, but not LIFRβ, protein levels in the sprouting SON at 10 days post lesion in the absence of neuronal loss. In contrast, osmotic stimulation of neurosecretory activity in the absence of injury resulted in a significant decrease in CNTF protein levels with no change in CNTFRα, gp130, or LIFRβ protein levels. Immunocytochemical analysis further demonstrated gp130 localization on magnocellular neurons and astrocytes while the LIFRβ receptor was found only on astrocytes in the SON. These results are consistent with the hypothesis that increased CNTF and CNTFR complex in the sprouting, metabolically active SON are related directly to the sprouting response and not the increase in neurosecretory activity.

Keywords

Activity-dependent; axonal sprouting; CNTFRα; CNTF; regulation; magnocellular neurosecretory system

Introduction

Collateral sprouting of axonal processes has been well documented in a variety of neuronal populations within the mature mammalian central nervous system (CNS). However, little is

Corresponding Author: John Watt, Room 1701 Stop 9037, 501 N Columbia Road, Grand Forks, ND 58203; phone: 701-777-6225; fax: 701-777-2477; john.watt@med.und.edu.

known about the factors that mediate collateral sprouting particularly in regards to the influence of neuronal activity on neurotrophin expression. The magnocellular neurosecretory system (MNS) is comprised of the vasopressinergic (VP) and oxytocinergic (OT) neurons located in the supraoptic (SON), paraventricular (PVN), and accessory hypothalamic nuclei and their projections via the hypothalamo-neurohypophysial tract to the neural lobe (NL) of the pituitary gland. We and others have demonstrated that the MNS provides an excellent model system with which to investigate the cellular mechanisms which underlie activity-dependant axonal reorganization (Morris and Dyball, 1974, Raisman, 1973, Silverman and Zimmerman, 1982, Watt, et al., 1999, Watt and Paden, 1991). Toward this end, we utilize a unilateral lesion of the hypothalamo-neurohypophysial tract in which the neurosecretory axons in the animal's right hemisphere PVN and SON are severed while the contralateral nuclei are spared (Watt and Paden, 1991). The lesion results in the loss of 42% of the neurosecretory axons in the NL followed by a return to control levels by four weeks post-lesion (Watt and Paden, 1991). The axonal recovery results from a collateral sprouting response arising from the non-injured, contralateral magnocellular neurons with a concomitant increase in; the magnocellular neuron somatic and nuclear area, oxytocin and vasopressin mRNA expression (Watt and Paden, 1991), and alpha-I and beta-II tubulin mRNA expression (Paden, et al., 1995). Daily measures of urine osmolality reveal a chronic hyperosmolality with a concomitant decrease in daily water intake and urine excretion volume, which persists throughout the post-surgical period. Together these results indicate that the sprouting event is not a compensatory response as it occurs in the absence of a functional deficit (Watt and Paden, 1991). Hence, the mechanism underlying the axonal sprouting remains undetermined.

Collateral sprouting has been shown to occur in a variety of neuronal populations; however, the factor or factors responsible for mediating the sprouting response are still largely ill defined. Ciliary neurotrophic factor (CNTF) has been implicated in hypothalamic magnocellular neuron sprouting *in vitro* (Vutskits, et al., 1998) and has been demonstrated to promote motor neuron sprouting (Gurney, et al., 1992, Guthrie, et al., 1997, Kwon and Gurney, 1994, Oyesiku and Wigston, 1996, Siegel, et al., 2000, Simon, et al., 2010, Ulenkate, et al., 1994, Wright, et al., 2007, Xu, et al., 2009). CNTF signals through the tripartite receptor complex consisting of the specific receptor for CNTF, CNTF receptor alpha (CNTFRα), and the gp130 and LIFRβ receptor subunits, to promote the survival of multiple neuronal phenotypes affected by injury across numerous species (Albrecht, et al., 2002, Arakawa, et al., 1990, Ip, et al., 1991, Larkfors, et al., 1994, Lehwalder, et al., 1989, Magal, et al., 1991, Sendtner, et al., 1990). Moreover, CNTF is a potent promoter of hypothalamic magnocellular neuron survival *in vitro* (House, et al., 2009, Rusnak, et al., 2002, Rusnak, et al., 2003, Vutskits, et al., 1998, Vutskits, et al., 2003). In our studies we have demonstrated an increase in CNTF-immunoreactivity (Watt, et al., 2006) and CNTFRα mRNA expression (Watt, et al., 2009) within the non-injured contralateral SON, which contains the sprouting and metabolically active magnocellular neurons. Together, these observations suggest that CNTF contributes to the axonal sprouting response. However, it remained to be determined if the observed increases CNTF and CNTFRα in the contralateral SON were related to the sprouting response per se or more generally to the increased neurosecretory activity associated with the post-lesion response. Therefore, the aim of the present study was to test the hypothesis that the observed increase in CNTF and CNTFRα in the SON contralateral to the unilateral lesion is related specifically to the onset of collateral axonal sprouting and not to the increase in neurosecretory activity which occurs concurrently with the sprouting event.

Experimental Procedures

Animals

Male Sprague-Dawley rats were purchased from Charles River Laboratories (Wilmington, MA) and housed in the University of North Dakota Center for Biomedical Research Facility, an AAALAC accredited facility, under a 12L:12D light cycle with ad lib access to lab chow and tap water throughout the investigations unless otherwise noted. Experimental protocols utilized in these studies followed the guidelines in the NIH guide for the care and use of laboratory animals and were approved by the UND Institutional Animal Care and Use Committee. Animals were 35–40 days of age (75–100g) at the time a unilateral hypothalamic knife cut of the hypothalamo-neurohypophysial tract was performed. The animals were secured in a stereotaxic apparatus (Stoelting, Wood Dale, IL) and kept under constant isoflurane anesthesia (2.5%; Abbot Laboratories; Abbott Park, IL) using a tabletop anesthesia apparatus (Matrx Quantiflex Low Flow V.M.C.; Matrx, Orchard Park, NY) equipped with an isoflurane Vaporizer (Matrx VIP 3000; Matrx). A wire knife constructed of HTX-33-gauge tubing was used to unilaterally transect the entire length of the hypothalamus through which the hypothalamo-neurohypophysial tract passes as previously described (Watt and Paden, 1991). The knife tract extended from the dorsal to the ventral surface of the brain, medial to the ipsilateral SON, but passing through the lateral aspect of the ipsilateral PVN. Stereotaxic lesion coordinates were 0.6 mm lateral to the midsagittal suture, and the lesion extended from −4.0 mm to +4.0 mm anterior-posterior from bregma. This results in complete transection of the ipsilateral hypothalamo-neurohypophysial tract. The animals were sacrificed 10 days post surgery along with age-matched non-injured control animals. All lesion tacks were confirmed histologically using cresyl violet. Only animals with a complete transection of the hypothalamo-neurohypophysial tract were included in these studies.

Male Sprague Dawley rats (200–250g) in the chronic salt-loaded groups were given 2% salt water substituted for tap water for 10 days prior to sacrifice. The animals were sacrificed with age-matched control animals. All efforts were made to minimize the numbers of animals used in this study and their suffering.

Gel electrophoresis and Western blot analysis

Following experimental periods, the animals were anesthetized with isoflurane, decapitated, and their brains were removed intact. SON samples were carefully collected under a dissecting microscope and pooled from 6 rats (30 total rats, n=5 groups of 6 pooled rat SON) in a solution of radioimmuno-precipitation assay (RIPA) buffer containing 20 mM Tris (pH 7.5 Sigma; St. Louis, MO), 150 mM NaCl (Sigma), 1% nonidet P-40 (Roche Diagnostics; Indianapolis, IN), 0.5% sodium deoxycholate (Sigma), 1 mM EDTA (Sigma), 0.1% SDS (Pierce; Rockford, IL), 1% protease inhibitor (Protease Inhibitor Cocktail; Sigma) and 1% phosphatase inhibitor (Phosphatase Inhibitor Cocktail 2; Sigma). The SON samples were then homogenized in RIPA buffer and centrifuged at 10,000 rpm for 20 minutes at 4°C. Supernatant from each sample was stored at −80°C until needed. SON protein content was determined using the bicinchoninic acid (BCA) colorimetric detection assay (Pierce BCA Protein Assay; Pierce). Each lane was loaded with 50 μg of protein and separated by a 12% SDS-PAGE gel (Precise Protein Gels; Pierce) at 90 V for approximately 1.5 hours and then electrophoretically transferred to a PVDF membrane (0.2 μm; Bio-Rad, Hercules, CA) at 70 V for 2 hours. After blocking non-specific binding sites (5% nonfat milk in phosphate-buffered saline (PBS) plus 0.1% Tween-20; blocking buffer; Bio-Rad), the membranes were incubated overnight at 4°C in rabbit anti-CNTF (1:5000; #AAR21, Serotec, Raleigh, NC). The membranes were then washed repeatedly for 1 hour in PBS-Tween and incubated for 2 hours in the appropriate HRP-conjugated secondary antibody (1:100,000; Santa Cruz

Biotechnology, Santa Cruz, CA). Following PBS washes for 2 hours, the bands were subsequently visualized using the West Femto chemiluminescent detection kit (Pierce) with high performance chemiluminescence film (Amersham Hyperfilm ECL; GE Healthcare; VWR; West Grove, PA) on an AGFA CP1000 film processor (DMS Health Group; Fargo, ND). Subsequently, bound antibodies were removed with stripping buffer (pH 2.2; 15g glycine; Sigma, 1 g SDS; Bio-Rad, 10 ml Tween-20; Bio-Rad in 1 L ultrapure water) for 10 minutes and the steps were repeated to sequentially reprobe the membrane for the following antibodies; mouse anti-CNTFRα (1:20,000; #558783, BD Biosciences, Franklin Lakes, NJ), rabbit anti-gp130 (1:5000; #sc-655, Santa Cruz Biotechnology,), rabbit anti-LIFRβ (1:5000; #sc-659, Santa Cruz Biotechnology), and mouse anti-β-actin (1:50,000; #A2228, Sigma).

Densitometric analysis of immunoblot signals was performed using MCID image analysis software (Version 7.0, Imaging Research Inc.). Briefly, digitized Western blot films were opened in MCID, bands of interest were outlined, with band area and relative optical densities (ROD) then determined. The area of the band was then multiplied by the density value. The ROD of all bands was normalized to the respective ROD of β-actin bands to obtain ratios. Analysis was repeated on 3 separate samples per group resulting in mean ratio values for each group that were used for statistical analysis as described below.

Immunocytochemistry

Animals were deeply anesthetized with isoflurane and perfused transcardially with 0.9% saline followed by periodate-lysine-paraformaldehyde fixative (PLP; 3.2% paraformaldehyde, 2.2% lysine, 0.33% sodium-(meta) periodate; Sigma) prepared immediately before use (McLean and Nakane, 1974). Brains were then removed and post-fixed overnight before cryoprotection in 20% sucrose in PBS. Serial cryosections (16 μm) were thaw-mounted on gelatin coated slides and stored at −20°C until further use.

Sections were washed with PBS containing 0.3% Triton X-100 (PBS-T; Sigma) in 3×10 minute intervals before and after all incubations. Non-specific staining was alleviated by treatment with 4% of the appropriate normal serum (Vector, Burlingame, CA) in PBS-T (blocking buffer) for 1 hour at room temperature followed by an overnight incubation at 4°C in guinea pig anti-OT (1:2000; #T-5021, Peninsula Laboratories, San Carlos, CA), guinea pig anti-VP (1:2000; #T-5048, Peninsula Laboratories), or goat anti-CNTF (1:100; #AF-557-NA, R&D Systems, Minneapolis, MN). Sections were then incubated in biotinylated donkey anti-guinea pig IgG (1:500; Vector) for 1 hour followed by incubation in avidin-biotin complex (ABC *Elite* kit, Vector). Binding of ABC reagent was visualized with a reaction in 0.05% diaminobenzidine (DAB; 200 mg glucose, 40 mg ammonium chloride, 50 mg DAB per 100 mL PBS; Sigma) using glucose oxidase (0.3%; Sigma) to generate hydrogen peroxide (Itoh, et al., 1979). Following PBS washes, sections labeled with anti-OT and anti-VP were counterstained with hematoxylin (Vector) for 30 seconds prior to dehydration in a graded series of alcohol.

For fluorescent immunocytochemical analysis, all steps were the same as listed above except incubation in Alexa strepavidin-488 (1:1000; Molecular Probes, Eugene, OR) followed by incubation in avidin-biotin complex. Sections prepared for fluorescent analysis were coverslipped with Vectashield mounting medium containing DAPI (Vector).

For dual-label fluorescence immunocytochemistry, all steps were the same as listed above unless otherwise noted. Tissue immunoreactivity was detected by incubation in a cocktail containing either rabbit anti-gp130 (1:200; #sc-655, Santa Cruz Biotechnology) or rabbit anti-LIFRβ (1:25; #sc-20752, Santa Cruz Biotechnology) with either mouse anti-GFAP (1:1000; #G-3893, Sigma), guinea pig anti-OT, or guinea pig anti-VP in blocking buffer overnight at 4°C followed by species-specific secondary IgG conjugated to either Alexa

Fluor 488 or Alexa Fluor 594 (1:100; Molecular Probes, Eugene, OR), respectively. Fluorescent sections were coverslipped with Vectashield mounting medium containing DAPI and examined using an Olympus BX-51 fluorescent microscope with attached DP-71 color camera and dedicated software.

As a control for the dual-label fluorescence immunocytochemistry, incubations with either rabbit anti-LIFRβ or rabbit anti-gp130 antibodies on separate sections of tissue were followed by an incubation with the species specific fluorescent-conjugated secondary antibodies for anti-GFAP, -OT, and -VP. Similarly, after separate sections of tissue were incubated with the anti-GFAP, -OT, or -VP antibodies the tissue was exposed to the fluorescent-conjugated secondary antibodies for the rabbit primary antibodies. These controls demonstrated an absence of immunoreactivity in the rat SON, indicating that the fluorescent-conjugated secondary antibodies were specific for their appropriate primary antibody and there was no observable cross-reactivity between the secondary antibodies.

Nuclear area measurements

To determine the area of the magnocellular neuron nuclei from salt-loaded and age-matched control SON, sections throughout the SON processed separately for anti-OT or anti-VP fluorescence were coded by a third-party blind to the experimental conditions. Merged digital images containing either the OT- or VP-immunoreactivity with the DAPI positive nucleus were obtained using an 40× objective on an Olympus BX51 microscope. The images were opened in Image J analysis software (NIH) and the outer edge of the DAPI positive nuclei containing nucleoli was traced in cells that were immunopositive for OT or VP in order to determine the area of the nuclei. Measures were repeated to include a minimum of 50 nuclei analyzed per animal per magnocellular neuron phenotype.

Vasopressin and oxytocin neuron counts

To ensure that the same magnocellular neuron was not counted twice, adjacent sections were stained for OT and VP magnocellular neurons and a minimum of five sections (80 μm) were skipped before the next section was processed. Following immunocytochemical labeling of oxytocinergic and vasopressinergic magnocellular neurons, the sections were randomly coded by a third-party blind to experimental conditions. Immunopositive neurons containing a counterstained nucleolus were counted using a drawing tube attached to an Olympus BX51 microscope. In order to account for the rostral-caudal size difference of the SON, we determined the numbers of cells per unit area of SON by obtaining the total area of each SON using Image J. Data are expressed as the percentage of the age-matched controls. A minimum of six sections containing a well defined SON were taken at rostral to caudal levels matched across animals for analysis

Statistical analysis

Distribution normality of each group of data was tested using the Kolmogorov-Smirnov test (GraphPad InStat, version 3.06 for Windows, San Diego California). Student's *t* test or one-way ANOVA with post *hoc* Tukey's tests (GraphPad InStat) were used, where appropriate, to compare groups with $p<0.05$ considered statistically significant. Results are expressed as the group means ± SEM.

Results

Protein levels of CNTF, CNTFRα, and gp130 are increased in the absence of injury in the sprouting, metabolically active SON

We demonstrated previously that unilateral lesion of the hypothalamo-neurohypophysial tract results in an increase in CNTF mRNA expression in the axotomized SON (Watt, et al.,

2006). This occurs concomitant with an increase in CNTF-immunoreactivity (Watt, et al., 2006) and CNTFRα mRNA expression (Watt, et al., 2009) in the contralateral, sprouting SON. However, the protein levels of CNTF and CNTFRα following unilateral lesion of the hypothalamo-neurohypophysial tract remained to be determined. Therefore, in the current study we quantified the protein levels of CNTF and components of the tripartite receptor complex, CNTFRα, gp130, and LIFRβ, in both the contralateral intact and axotomized SON and sought to determine if the responses in the contralateral SON are due to increased neurosecretory activity.

As shown in Fig. 1A, Western blot analysis revealed a band at approximately 23 kDa corresponding to CNTF in the control SON indicating endogenous expression in the absence of injury. By ten days post lesion (10 dpl) Western blot analysis further demonstrated that CNTF protein levels were significantly elevated by 131% in the SON contralateral to the injury (Fig. 1A; one-way ANOVA, $p<0.0001$) and by 247% in the axotomized SON compared to age-matched control SON (Fig. 1A; one-way ANOVA, $p<0.0001$). Protein levels of CNTFRα undergo similar changes in the SON following unilateral lesion. As shown in Fig. 1B, in the non-injured control SON, low endogenous CNTFRα protein levels were detectable by Western blot analysis with a small and faint band at approximately 60 kDa corresponding to CNTFRα (Fig. 1B). However, by 10 dpl we observed a 288% increase in CNTFRα protein levels in the SON contralateral to the injury and a 437% increase in the axotomized SON compared to age-matched control SON (Fig. 1B; one-way ANOVA, $p<0.0001$).

CNTF-mediated intracellular signaling is conducted via the tripartite receptor complex consisting of CNTFRα, gp130, and LIFRβ (Davis, et al., 1993). While CNTFRα provides the specificity for CNTF signaling, it is the gp130 and LIFRβ components that directly mediate intracellular signaling in response to CNTF (Davis, et al., 1993). Therefore, we next examined whether the changes in CNTFRα were accompanied by changes in gp130 and LIFRβ protein levels. As shown in Fig. 1C, Western blot analysis demonstrated a faint band at approximately 130 kDa corresponding to gp130 in the non-injured control SON (Fig. 1C). By 10 dpl protein levels of gp130 increased by 176% in the SON contralateral to the injury and 258% in the axotomized SON compared to age-matched control SON (Fig. 1C; one-way ANOVA, $p<0.0001$). In contrast, LIFRβ protein levels in the SON contralateral to the injury were not significantly different than age-matched control levels at 10 dpl, although the unilateral lesion did result in a significant increase of 82% in the LIFRβ protein levels in the axotomized SON compared to age-matched control SON (Fig. 1D; one-way ANOVA, $p<0.0001$).

In order to determine if the increases in CNTF, CNTFRα, and gp130 protein levels in the SON contralateral to the injury, from which the collateral sprouting response arises, are not due to a loss of magnocellular neurons in the contralateral SON, cell counts of immunolabeled OT and VP magnocellular neurons were performed. Our results demonstrate that there was no decrease in the number of OT or VP magnocellular neurons in the SON contralateral to the unilateral lesion (Fig. 2). However, hypothalamic unilateral lesion did result in the loss of 85% of the oxytocinergic and 90% of the vasopressinergic magnocellular neurons in the axotomized SON (Fig. 2; one-way ANOVA, $p<0.0001$).

Taken together, these data demonstrate that the injury associated with unilateral hypothalamic lesion increased the protein levels of CNTF and its receptor components in the axotomized SON in spite of an almost complete loss of magnocellular neurons. These data demonstrate that CNTF and a complete, presumably functional, receptor complex are expressed by SON astrocytes indicating an autocrine signaling mechanism. Furthermore, protein levels of CNTF and its receptor components are significantly elevated in the

sprouting, metabolically active SON, in the absence of neuronal loss, suggesting that either the sprouting response per se or the increase in neurosecretory activity resulted in the increase in the protein levels of CNTF and its receptor components.

Increased neurosecretory activity results in decreased CNTF protein levels in the SON

In order to determine how physiological activation of the magnocellular neurosecretory system affects CNTF, CNTFRα, gp130, and LIFRβ protein levels in the SON, we utilized a chronic hypernatremia paradigm in which non-injured magnocellular neurons are physiologically activated for 10 days by substituting tap water with a 2% salt water solution. Previous reports have demonstrated that physiological activation of the MNS via salt loading results in heightened neurosecretory output and synthetic activity which is reflected in increased size of magnocellular somata and nuclei of in the SON (Hatton and Walters, 1973, Lin, et al., 1996, Theodosis and Poulain, 1984, Watt, et al., 1999). Consistent with those reports, we demonstrated a significant hypertrophy of 25% and 32% in oxytocinergic and vasopressinergic magnocellular neuron nuclei area, respectively, in the salt-loaded SON (Fig. 3; Student's *t*-test, $p<0.0001$). These data demonstrate that 10 days of chronic salt-loading successfully induces physiological activation of the magnocellular neurons of the SON. Quantitative Western blot analysis was then performed to determine CNTF, CNTFRα, gp130, and LIFRβ protein levels in the SON following physiological activation.

In contrast to our observations in the axotomized and contralateral sprouting SON, our Western blot analysis revealed a significant decrease in CNTF protein levels in the salt-loaded SON compared to the age-matched control SON from animals maintained on tap water (Fig. 4A; Student's t-test, $p<0.001$). These results were further illustrated in sections of SON immunolabeled for CNTF which show that the CNTF-immunoreactivity, which is highly localized to GFAP-immunoreactive astrocytes residing in the ventral glial-limitans (VGL) of the SON (Watt, et al., 2006), is appreciably more prominent and extensive in its projections through the SON than the CNTF-immunoreactivity in the salt-loaded SON (compare Figs. 4B, C). Western blot analysis demonstrated no significant difference between CNTFRα (Fig. 5A), gp130 (Fig. 5B), or LIFRβ (Fig. 5C) protein levels in the salt-loaded SON and the age-matched control SON. Thus, these data demonstrate that an increase in neurosecretory activity in the absence of injury does not result in increased CNTF or CNTF receptor component protein levels as was observed in the sprouting SON contralateral to unilateral lesion of the hypothalamo-neurohypophysial tract. Furthermore, these data are the first evidence of an activity-dependent change, in the absence of injury, in CNTF protein levels in the CNS.

gp130-immunoreactivity is localized to magnocellular neurons and astrocytes while LIFRβ-immunoreactivity is localized to astrocytes of the SON

We performed immunocytochemical analysis of gp130 and LIFRβ localization to identify cell phenotypes that express these receptors within the SON. We observed robust immunoreactivity for gp130 on neuronal somata distributed throughout the SON (Figs. 6A–F), suggesting that virtually all magnocellular neurons in the SON express the protein. Dual-label immunocytochemistry confirmed the presence of gp130-immunoreactivity associated with both VP (Figs. 6A–C) and OT (not shown) magnocellular neurons. We also observed gp130-immunoreactivity localized to GFAP-immunoreactive astrocytes in the VGL of the SON (Figs. 6D–F).

In contrast to gp-130-immunoreactivity, we did not observe any LIFRβ-immunoreactive profiles that were consistent with neuronal somata (Figs. 6G–I). However, we did observe a strong band of LIFRβ-immunoreactivity in the VGL of the SON (Figs. 6G–L). Dual-label immunocytochemistry demonstrated that the astrocytes of the SON (Figs. 6J–L) contain the

LIFRβ protein and that vasopressinergic (Figs. 6G–I) and oxytocinergic (not shown) magnocellular neurons do not contain the LIFRβ protein.

Discussion

The present observations confirm and extend our previous reports demonstrating an increase in CNTF-immunoreactivity and CNTFRα mRNA expression in the contralateral sprouting SON (Watt, et al., 2006, Watt, et al., 2009). This increase in CNTF and its receptor occurs during the period when a robust collateral sprouting of intact neurosecretory axons is occurring in response to partial denervation of the NL (Watt, et al., 1999, Watt and Paden, 1991). CNTF is of particular interest with regard to axonal sprouting due to its demonstrated effects on sprouting in the central and peripheral nervous systems. Numerous reports have demonstrated that CNTF promotes motor neuron sprouting (Gurney, et al., 1992, Kwon and Gurney, 1994, Oyesiku and Wigston, 1996, Siegel, et al., 2000, Simon, et al., 2010, Ulenkate, et al., 1994, Wright, et al., 2007, Xu, et al., 2009). In addition, CNTF was previously implicated in hypothalamic MCN process outgrowth *in vitro* (Vutskits, et al., 1998). Consistent with our results, others have demonstrated an increase in astrocytic CNTF and CNTFRα expression during the period of entorhinal cortex (Lee, et al., 1997) and hippocampal (Guthrie, et al., 1997) sprouting, providing further evidence for a direct involvement of CNTF in promoting post-injury axonal sprouting.

Activity-dependent regulation of CNTF in the SON

In our previous studies we demonstrated that the cross sectional area of OT and VP somata and nuclei are significantly increased in the sprouting SON by ten days and 30 days post lesion, respectively (Watt, et al., 1999). This hypertrophy was accompanied by increased neurosecretory activity as evidenced by a persistent increase in urine osmolality accompanied by decreased urine volume and water intake beginning 3 days following unilateral lesion and maintained throughout the sprouting event (Watt and Paden, 1991). These data lead us to hypothesize that collateral sprouting by intact magnocellular neurons occurs as a direct response to increased activity rather than as a consequence of partial denervation in the NL. This possibility is supported by studies demonstrating that the survival and collateral axonal sprouting of OT and VP neurons after axotomy is attenuated by decreased neuronal activity (Dohanics, et al., 1996, Herman, et al., 1987, Shahar, et al., 2004, Watt, et al., 1999) and by evidence of increased magnocellular survival in response to KCL stimulation (Shahar, et al., 2004) and chronic intermittent salt loading (Huang and Dellmann, 1996). Key to understanding the interaction between increased activity and collateral sprouting is to determine the responses of various growth factors to these events. The hypothesis that increased neuronal activity may be sufficient in itself to induce changes in expression levels of CNTF and the CNTF receptor is supported by evidence for activity-induced changes in BDNF mRNA expression in neurons in the PVN (Castren, et al., 1995) and SON (Aliaga, et al., 2002) following osmotic stimulation. Indeed, our data show that heightened metabolic activity in the absence of the post-denervation sprouting response resulted in a significant decrease in CNTF protein levels within the SON, but with no measureable change in CNTFRα, LIFRβ, or gp-130 protein levels. However, it remains to be determined whether the decrease in CNTF protein levels results from a down-regulation in CNTF message levels or increased secretion as these two events would have predictably different effects on neurosecretory behavior.

The expression of CNTF and the CNTF-receptor complex by SON astrocytes indicate that astrocyte-derived CNTF acts through an autocrine signaling mechanism to promote indirectly magnocellular survival and axonal sprouting. This is further evidenced by our data showing the absence of LIFRβ-immunoreactivity on magnocellular neurons which would preclude receptor-mediated signaling in response to CNTF. These data are consistent with

the observations of Rusnak, et al. (2003) who indicated that addition of CNTF to dissociated cultures of magnocellular neurons did not result in increased neuronal survival. However, when CNTF is applied to stationary organotypic cultures of the SON and PVN, survival of axotomized magnocellular neurons is increased significantly (House, et al., 2009, Rusnak, et al., 2002, Rusnak, et al., 2003, Vutskits, et al., 1998, Vutskits, et al., 2003) indicating that CNTF is acting through astrocytes or other glial elements. The precise mechanism(s) by which CNTF influences neuronal survival and axonal sprouting remains unclear. However, CNTF induces increased expression of GFAP (Kahn, et al., 1997) and morphological alterations in astrocytes *in vivo* (Lisovoski, et al., 1997). SON astrocytes are highly plastic and modulate neurosecretory activity in part by altering their process morphology to facilitate increased neuron to neuron contact (Bobak and Salm, 1996, Salm and Hawrylak, 2004). Thus, the activity-dependant decrease in CNTF levels observed herein may influence magnocellular behavior indirectly through decreased astrocyte GFAP synthesis and process retraction. Alternatively, CNTF may influence axonal sprouting by stimulating production of other factors known to influence process outgrowth including fibroblast growth factor-2 (FGF-2) and nerve growth factor (NGF) (Albrecht, et al., 2002, Jiang, et al., 1999, Semkova and Krieglstein, 1999, Wang, et al., 2008). Heightened neuronal activity has been demonstrated to modulate neurotrophin expression throughout the brain, such as increases in hippocampal brain-derived neurotrophic factor (BDNF) during seizure (Katoh-Semba, et al., 1999) and physical activity (Neeper, et al., 1996). Likewise, increased expression of BDNF and its secretion from dendrites of magnocellular neurons in the SON has been reported in salt-loaded rats (Aliaga, et al., 2002, Arancibia, et al., 2007).

Increased excitatory afferent input may also modulate CNTF expression in the SON. The SON is the main target for the noradrenergic system arising from the brainstem (Cunningham and Sawchenko, 1988, Sawchenko and Swanson, 1981). During states of heightened neurosecretory activity, noradrenaline, via the α_1-adrenoreceptor, plays a critical excitatory role in the release of OT and VP from magnocellular neurons (Armstrong, et al., 1986, Leibowitz, et al., 1990, Willoughby, et al., 1987). Within the SON, the majority of adrenergic varicosities are found ventral to the magnocellular cell bodies in the dendritic zone (McNeill and Sladek, 1980, Swanson, et al., 1981). The dendritic zone is the location of the magnocellular neuron dendrites and astrocyte processes (Armstrong, et al., 1982, Dyball and Kemplay, 1982, Yulis, et al., 1984) and adrenergic receptors are expressed on astrocytes of the SON (Lafarga, et al., 1992). In addition, reports have demonstrated that noradrenaline decreases CNTF mRNA expression and protein levels when applied to cultured astrocytes (Carroll, et al., 1993, Rudge, et al., 1994). Collectively, these reports suggest that during states of heightened neurosecretory activity in the SON, increased noradrenergic stimulation results in down-regulation of CNTF protein levels in the SON. Future experiments will test this hypothesis by analyzing CNTF protein levels following chronic infusion of adrenergic receptor agonists and antagonists into the SON *in vivo*.

Conclusions

In conclusion, we provide the first evidence for activity-dependent regulation of CNTF in the CNS in the absence of injury. In addition, our data demonstrate that the increase in CNTF and CNTF-receptor complex observed in the sprouting SON is related to the sprouting response per se and not to the increased neurosecretory activity associated with the post-lesion response. Furthermore, the absence of immunoreactivity for the LIFRβ component of the CNTF receptor complex on magnocellular neurons provide further support to the hypothesis that CNTF is acting through an autocrine mechanism to enhance, indirectly, neuronal survival and axonal sprouting of magnocellular neurons. Together, these data provide strong support for our hypothesis that the increase in CNTF/CNTFRα observed

is specifically related to the axonal sprouting response and supports neuronal sprouting through an astrocyte-dependent paracrine mechanism.

Highlights

> Increased neuronal activity decreases CNTF but not CNTF receptor protein levels. > CNTF and CNTF receptor levels increase in metabolically active sprouting neurons. > Increased CNTF and CNTF receptor expression is directly linked to axonal sprouting.

Abbreviations

CNTF	ciliary neurotrophic factor
CNTFRα	ciliary neurotrophic factor receptor alpha
LIFRβ	leukocyte inhibitory factor receptor beta
SON	supraoptic nucleus
PVN	paraventricular nucleus
VP	vasopressinergic
OT	oxytocinergic
NL	neural lobe
ROD	relative optical density
GFAP	glial fibrillary acidic protein
VGL	ventral glial limitans
BDNF	brain derived neurotrophic factor
FGF	fibroblast growth factor
NGF	nerve growth factor

Acknowledgments

This publication was made possible by grant number P20RR017699 from the National Center for Research Resources (NCRR), a component of the National Institutes of Health (NIH). The authors wish to thank Dr. Catherine Brissette for her helpful comments during the preparation of this manuscript.

References

1. Albrecht PJ, Dahl JP, Stoltzfus OK, Levenson R, Levison SW. Ciliary neurotrophic factor activates spinal cord astrocytes, stimulating their production and release of fibroblast growth factor-2, to increase motor neuron survival. Exp Neurol. 2002; 173:46–62. [PubMed: 11771938]
2. Aliaga E, Arancibia S, Givalois L, Tapia-Arancibia L. Osmotic stress increases brain-derived neurotrophic factor messenger RNA expression in the hypothalamic supraoptic nucleus with differential regulation of its transcripts. Relation to arginine-vasopressin content. Neuroscience. 2002; 112:841–850. [PubMed: 12088743]
3. Arakawa Y, Sendtner M, Thoenen H. Survival effect of ciliary neurotrophic factor (CNTF) on chick embryonic motoneurons in culture: comparison with other neurotrophic factors and cytokines. J Neurosci. 1990; 10:3507–3515. [PubMed: 2230940]
4. Arancibia S, Lecomte A, Silhol M, Aliaga E, Tapia-Arancibia L. In vivo brain-derived neurotrophic factor release and tyrosine kinase B receptor expression in the supraoptic nucleus after osmotic stress stimulus in rats. Neuroscience. 2007; 146:864–873. [PubMed: 17346893]

5. Armstrong WE, Gallagher MJ, Sladek CD. Noradrenergic stimulation of supraoptic neuronal activity and vasopressin release in vitro: mediation by an alpha 1-receptor. Brain Res. 1986; 365:192–197. [PubMed: 3004655]
6. Armstrong WE, Scholer J, McNeill TH. Immunocytochemical, Golgi and electron microscopic characterization of putative dendrites in the ventral glial lamina of the rat supraoptic nucleus. Neuroscience. 1982; 7:679–694. [PubMed: 6175923]
7. Bobak JB, Salm AK. Plasticity of astrocytes of the ventral glial limitans subjacent to the supraoptic nucleus. J Comp Neurol. 1996; 376:188–197. [PubMed: 8951636]
8. Carroll P, Sendtner M, Meyer M, Thoenen H. Rat ciliary neurotrophic factor (CNTF): gene structure and regulation of mRNA levels in glial cell cultures. Glia. 1993; 9:176–187. [PubMed: 8294148]
9. Castren E, Thoenen H, Lindholm D. Brain-derived neurotrophic factor messenger RNA is expressed in the septum, hypothalamus and in adrenergic brain stem nuclei of adult rat brain and is increased by osmotic stimulation in the paraventricular nucleus. Neuroscience. 1995; 64:71–80. [PubMed: 7708216]
10. Cunningham ET Jr. Sawchenko PE. Anatomical specificity of noradrenergic inputs to the paraventricular and supraoptic nuclei of the rat hypothalamus. J Comp Neurol. 1988; 274:60–76. [PubMed: 2458397]
11. Davis S, Aldrich TH, Stahl N, Pan L, Taga T, Kishimoto T, Ip NY, Yancopoulos GD. LIFR beta and gp130 as heterodimerizing signal transducers of the tripartite CNTF receptor. Science. 1993; 260:1805–1808. [PubMed: 8390097]
12. Dohanics J, Hoffman GE, Verbalis JG. Chronic hyponatremia reduces survival of magnocellular vasopressin and oxytocin neurons after axonal injury. J Neurosci. 1996; 16:2373–2380. [PubMed: 8601817]
13. Dyball RE, Kemplay SK. Dendritic trees of neurones in the rat supraoptic nucleus. Neuroscience. 1982; 7:223–230. [PubMed: 7078727]
14. Gurney ME, Yamamoto H, Kwon Y. Induction of motor neuron sprouting in vivo by ciliary neurotrophic factor and basic fibroblast growth factor. J Neurosci. 1992; 12:3241–3247. [PubMed: 1494954]
15. Guthrie KM, Woods AG, Nguyen T, Gall CM. Astroglial ciliary neurotrophic factor mRNA expression is increased in fields of axonal sprouting in deafferented hippocampus. J Comp Neurol. 1997; 386:137–148. [PubMed: 9303530]
16. Hatton GI, Walters JK. Induced multiple nucleoli, nucleolar margination, and cell size changes in supraoptic neurons during dehydration and rehydration in the rat. Brain Res. 1973; 59:137–154. [PubMed: 4747747]
17. Herman JP, Marciano FF, Wiegand SJ, Gash DM. Selective cell death of magnocellular vasopressin neurons in neurohypophysectomized rats following chronic administration of vasopressin. J Neurosci. 1987; 7:2564–2575. [PubMed: 3302129]
18. House SB, Li C, Yue C, Gainer H. Effects of ciliary neurotrophic factor and leukemia inhibiting factor on oxytocin and vasopressin magnocellular neuron survival in rat and mouse hypothalamic organotypic cultures. J Neurosci Methods. 2009; 178:128–133. [PubMed: 19118574]
19. Huang YS, Dellmann HD. Chronic intermittent salt loading enhances functional recovery from polydipsia and survival of vasopressinergic cells in the hypothalamic supraoptic nucleus following transection of the hypophysial stalk. Brain Res. 1996; 732:95–105. [PubMed: 8891273]
20. Ip NY, Li YP, van de Stadt I, Panayotatos N, Alderson RF, Lindsay RM. Ciliary neurotrophic factor enhances neuronal survival in embryonic rat hippocampal cultures. J Neurosci. 1991; 11:3124–3134. [PubMed: 1941077]
21. Itoh K, Konishi A, Nomura S, Mizuno N, Nakamura Y, Sugimoto T. Application of coupled oxidation reaction to electron microscopic demonstration of horseradish peroxidase: cobalt-glucose oxidase method. Brain Res. 1979; 175:341–346. [PubMed: 90544]
22. Jiang F, Levison SW, Wood TL. Ciliary neurotrophic factor induces expression of the IGF type I receptor and FGF receptor 1 mRNAs in adult rat brain oligodendrocytes. J Neurosci Res. 1999; 57:447–457. [PubMed: 10440894]

23. Kahn MA, Ellison JA, Chang RP, Speight GJ, de Vellis J. CNTF induces GFAP in a S-100 alpha brain cell population: the pattern of CNTF-alpha R suggests an indirect mode of action. Brain Res Dev Brain Res. 1997; 98:221–233.
24. Katoh-Semba R, Takeuchi IK, Inaguma Y, Ito H, Kato K. Brain-derived neurotrophic factor, nerve growth and neurotrophin-3 selected regions of the rat brain following kainic acid-induced seizure activity. Neurosci Res. 1999; 35:19–29. [PubMed: 10555160]
25. Kwon YW, Gurney ME. Systemic injections of ciliary neurotrophic factor induce sprouting by adult motor neurons. Neuroreport. 1994; 5:789–792. [PubMed: 8018851]
26. Lafarga M, Berciano MT, Del Olmo E, Andres MA, Pazos A. Osmotic stimulation induces changes in the expression of beta-adrenergic receptors and nuclear volume of astrocytes in supraoptic nucleus of the rat. Brain Res. 1992; 588:311–316. [PubMed: 1327410]
27. Larkfors L, Lindsay RM, Alderson RF. Ciliary neurotrophic factor enhances the survival of Purkinje cells in vitro. Eur J Neurosci. 1994; 6:1015–1025. [PubMed: 7952272]
28. Lee MY, Deller T, Kirsch M, Frotscher M, Hofmann HD. Differential regulation of ciliary neurotrophic factor (CNTF) and CNTF receptor alpha expression in astrocytes and neurons of the fascia dentata after entorhinal cortex lesion. J Neurosci. 1997; 17:1137–1146. [PubMed: 8994067]
29. Lehwalder D, Jeffrey PL, Unsicker K. Survival of purified embryonic chick retinal ganglion cells in the presence of neurotrophic factors. J Neurosci Res. 1989; 24:329–337. [PubMed: 2585553]
30. Leibowitz SF, Eidelman D, Suh JS, Diaz S, Sladek CD. Mapping study of noradrenergic stimulation of vasopressin release. Exp Neurol. 1990; 110:298–305. [PubMed: 2249740]
31. Lin SH, Miyata S, Kawarabayashi T, Nakashima T, Kiyohara T. Hypertrophy of oxytocinergic magnocellular neurons in the hypothalamic supraoptic nucleus from gestation to lactation. Zoolog Sci. 1996; 13:161–165. [PubMed: 8688810]
32. Lisovoski F, Akli S, Peltekian E, Vigne E, Haase G, Perricaudet M, Dreyfus PA, Kahn A, Peschanski M. Phenotypic alteration of astrocytes induced by ciliary neurotrophic factor in the intact adult brain, As revealed by adenovirus-mediated gene transfer. J Neurosci. 1997; 17:7228–7236. [PubMed: 9295369]
33. Magal E, Burnham P, Varon S. Effect of CNTF on low-affinity NGF receptor expression by cultured neurons from different rat brain regions. J Neurosci Res. 1991; 30:560–566. [PubMed: 1666130]
34. McLean IW, Nakane PK. Periodate-lysine-paraformaldehyde fixative. A new fixation for immunoelectron microscopy. J Histochem Cytochem. 1974; 22:1077–1083. [PubMed: 4374474]
35. McNeill TH, Sladek JR Jr. Simultaneous monoamine histofluorescence and neuropeptide immunocytochemistry: II. Correlative distribution of catecholamine varicosities and magnocellular neurosecretory neurons in the rat supraoptic and paraventricular nuclei. J Comp Neurol. 1980; 193:1023–1033. [PubMed: 7000861]
36. Morris JF, Dyball RE. A quantitative study of the ultrastructural changes in the hypothalamo-neurohypophysial system during and after experimentally induced hypersecretion. Cell Tissue Res. 1974; 149:525–535. [PubMed: 4367857]
37. Neeper SA, Gomez-Pinilla F, Choi J, Cotman CW. Physical activity increases mRNA for brain-derived neurotrophic factor and nerve growth factor in rat brain. Brain Res. 1996; 726:49–56. [PubMed: 8836544]
38. Oyesiku NM, Wigston DJ. Ciliary neurotrophic factor stimulates neurite outgrowth from spinal cord neurons. J Comp Neurol. 1996; 364:68–77. [PubMed: 8789276]
39. Paden CM, Zhou X, Watt JA, Burton R, Pickett J, Oblinger MM. Coordinated upregulation of alpha 1- and beta II-tubulin mRNAs during collateral axonal sprouting of central peptidergic neurons. J Neurosci Res. 1995; 42:402–412. [PubMed: 8583509]
40. Raisman G. Electron microscopic studies of the development of new neurohaemal contacts in the median eminence of the rat after hypophysectomy. Brain Res. 1973; 55:245–261. [PubMed: 4714005]
41. Rudge JS, Morrissey D, Lindsay RM, Pasnikowski EM. Regulation of ciliary neurotrophic factor in cultured rat hippocampal astrocytes. Eur J Neurosci. 1994; 6:218–229. [PubMed: 8167843]

42. Rusnak M, House SB, Arima H, Gainer H. Ciliary neurotrophic factor increases the survival of magnocellular vasopressin and oxytocin neurons in rat supraoptic nucleus in organotypic cultures. Microsc Res Tech. 2002; 56:101–112. [PubMed: 11810713]
43. Rusnak M, House SB, Gainer H. Long-term effects of ciliary neurotrophic factor on the survival of vasopressin magnocellular neurones in the rat supraoptic nucleus in vitro. J Neuroendocrinol. 2003; 15:933–939. [PubMed: 12969237]
44. Salm AK, Hawrylak N. Glial limitans elasticity subjacent to the supraoptic nucleus. J Neuroendocrinol. 2004; 16:661–668. [PubMed: 15271058]
45. Sawchenko PE, Swanson LW. Central noradrenergic pathways for the integration of hypothalamic neuroendocrine and autonomic responses. Science. 1981; 214:685–687. [PubMed: 7292008]
46. Semkova I, Krieglstein J. Ciliary neurotrophic factor enhances the expression of NGF and p75 low-affinity NGF receptor in astrocytes. Brain Res. 1999; 838:184–192. [PubMed: 10446331]
47. Sendtner M, Kreutzberg GW, Thoenen H. Ciliary neurotrophic factor prevents the degeneration of motor neurons after axotomy. Nature. 1990; 345:440–441. [PubMed: 2342575]
48. Shahar T, House SB, Gainer H. Neural activity protects hypothalamic magnocellular neurons against axotomy-induced programmed cell death. J Neurosci. 2004; 24:6553–6562. [PubMed: 15269267]
49. Siegel SG, Patton B, English AW. Ciliary neurotrophic factor is required for motoneuron sprouting. Exp Neurol. 2000; 166:205–212. [PubMed: 11085886]
50. Silverman AJ, Zimmerman EA. Adrenalectomy increases sprouting in a peptidergic neurosecretory system. Neuroscience. 1982; 7:2705–2714. [PubMed: 7155347]
51. Simon CM, Jablonka S, Ruiz R, Tabares L, Sendtner M. Ciliary neurotrophic factor-induced sprouting preserves motor function in a mouse model of mild spinal muscular atrophy. Hum Mol Genet. 2010; 19:973–986. [PubMed: 20022887]
52. Swanson LW, Sawchenko PE, Berod A, Hartman BK, Helle KB, Vanorden DE. An immunohistochemical study of the organization of catecholaminergic cells and terminal fields in the paraventricular and supraoptic nuclei of the hypothalamus. J Comp Neurol. 1981; 196:271–285. [PubMed: 6111572]
53. Theodosis DT, Poulain DA. Evidence for structural plasticity in the supraoptic nucleus of the rat hypothalamus in relation to gestation and lactation. Neuroscience. 1984; 11:183–193. [PubMed: 6709185]
54. Ulenkate HJ, Kaal EC, Gispen WH, Jennekens FG. Ciliary neurotrophic factor improves muscle fibre reinnervation after facial nerve crush in young rats. Acta Neuropathol. 1994; 88:558–564. [PubMed: 7879603]
55. Vutskits L, Bartanusz V, Schulz MF, Kiss JZ. Magnocellular vasopressinergic neurons in explant cultures are rescued from cell death by ciliary neurotrophic factor and leukemia inhibiting factor. Neuroscience. 1998; 87:571–582. [PubMed: 9758224]
56. Vutskits L, Gascon E, Kiss JZ. Removal of PSA from NCAM affects the survival of magnocellular vasopressin- and oxytocin-producing neurons in organotypic cultures of the paraventricular nucleus. Eur J Neurosci. 2003; 17:2119–2126. [PubMed: 12786978]
57. Wang X, Zheng H, Liu C, Zhu C, Wang W, Li Z. Ciliary neurotrophic factor-treated astrocyte conditioned medium regulates the L-type calcium channel activity in rat cortical neurons. Neurochem Res. 2008; 33:826–832. [PubMed: 17940876]
58. Watt JA, Bone S, Pressler M, Cranston HJ, Paden CM. Ciliary neurotrophic factor is expressed in the magnocellular neurosecretory system of the rat in vivo: evidence for injury- and activity-induced upregulation. Exp Neurol. 2006; 197:206–214. [PubMed: 16226750]
59. Watt JA, Lo D, Cranston HJ, Paden CM. CNTF receptor alpha is expressed by magnocellular neurons and expression is upregulated in the rat supraoptic nucleus during axonal sprouting. Exp Neurol. 2009; 215:135–141. [PubMed: 18973757]
60. Watt JA, Moffet CW, Zhou X, Short S, Herman JP, Paden CM. Central peptidergic neurons are hyperactive during collateral sprouting and inhibition of activity suppresses sprouting. J Neurosci. 1999; 19:1586–1598. [PubMed: 10024346]

61. Watt JA, Paden CM. Compensatory sprouting of uninjured magnocellular neurosecretory axons in the rat neural lobe following unilateral hypothalamic lesion. Exp Neurol. 1991; 111:9–24. [PubMed: 1984437]

62. Willoughby JO, Jervois PM, Menadue MF, Blessing WW. Noradrenaline, by activation of alpha-1-adrenoceptors in the region of the supraoptic nucleus, causes secretion of vasopressin in the unanaesthetized rat. Neuroendocrinology. 1987; 45:219–226. [PubMed: 3031526]

63. Wright MC, Cho WJ, Son YJ. Distinct patterns of motor nerve terminal sprouting induced by ciliary neurotrophic factor vs. botulinum toxin. J Comp Neurol. 2007; 504:1–16. [PubMed: 17614103]

64. Xu JJ, Chen EY, Lu CL, He C. Recombinant ciliary neurotrophic factor promotes nerve regeneration and induces gene expression in silicon tube-bridged transected sciatic nerves in adult rats. J Clin Neurosci. 2009; 16:812–817. [PubMed: 19289286]

65. Yulis CR, Peruzzo B, Rodriguez EM. Immunocytochemistry and ultrastructure of the neuropil located ventral to the rat supraoptic nucleus. Cell Tissue Res. 1984; 236:171–180. [PubMed: 6713504]

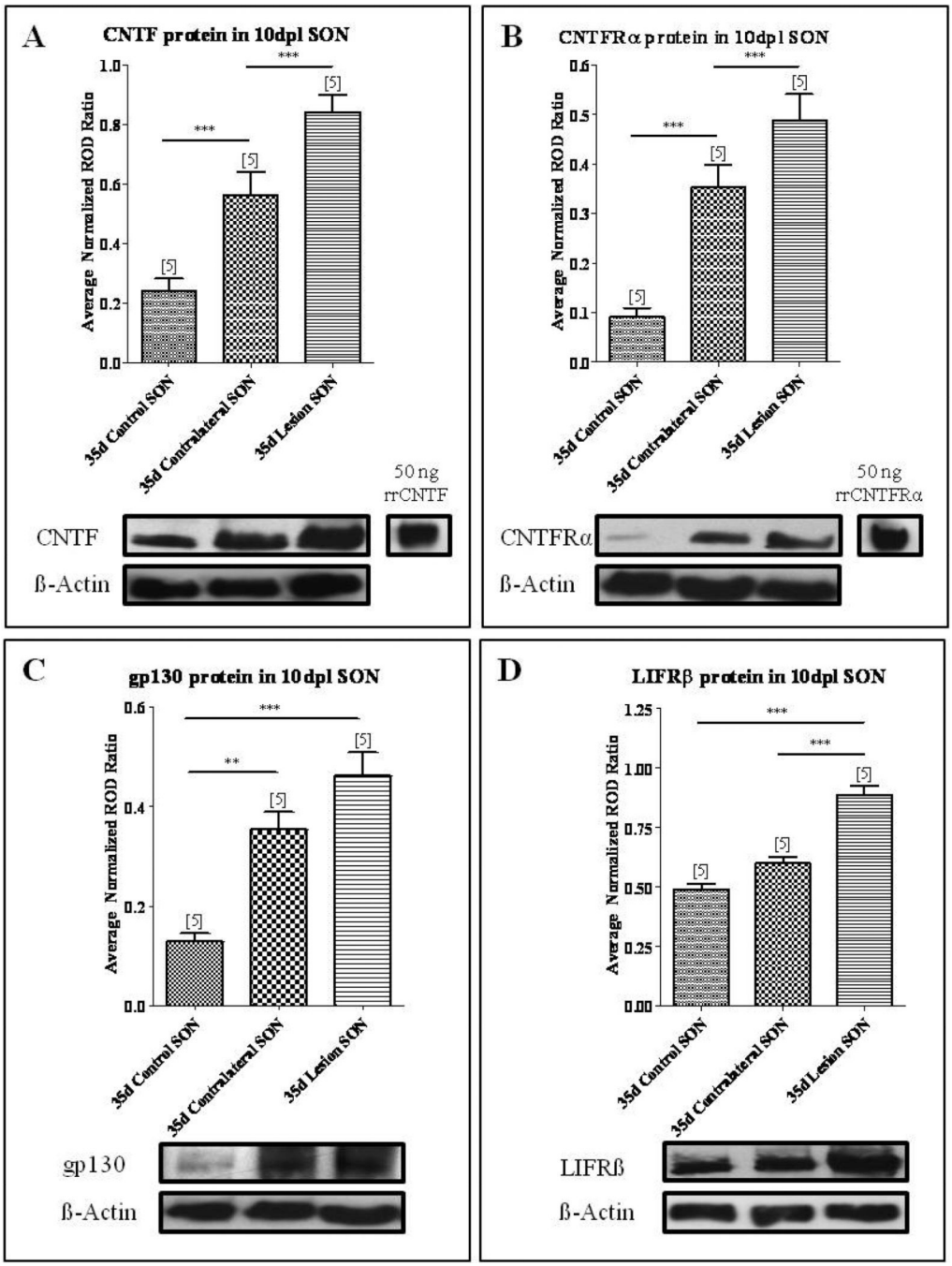

Fig. 1. CNTF and CNTF receptor complex are increased following axotomy

Western blot analysis demonstrated a significant increase in CNTF (A), CNTFRα (B), gp130 (C), and LIFRβ (D) protein levels in the axotomized SON compared to age-matched control. Within the sprouting SON contralateral to the lesion, CNTF (A), CNTFRα (B), and gp130 (C) protein levels were significantly increased compared to age-matched control. However, LIFRβ levels were not significantly changed. Column bars and error bars represent the mean and SEM of 5 groups. Each group represents isolated SON pooled from six rats. ***p<0.01*, ****p<0.0001*.

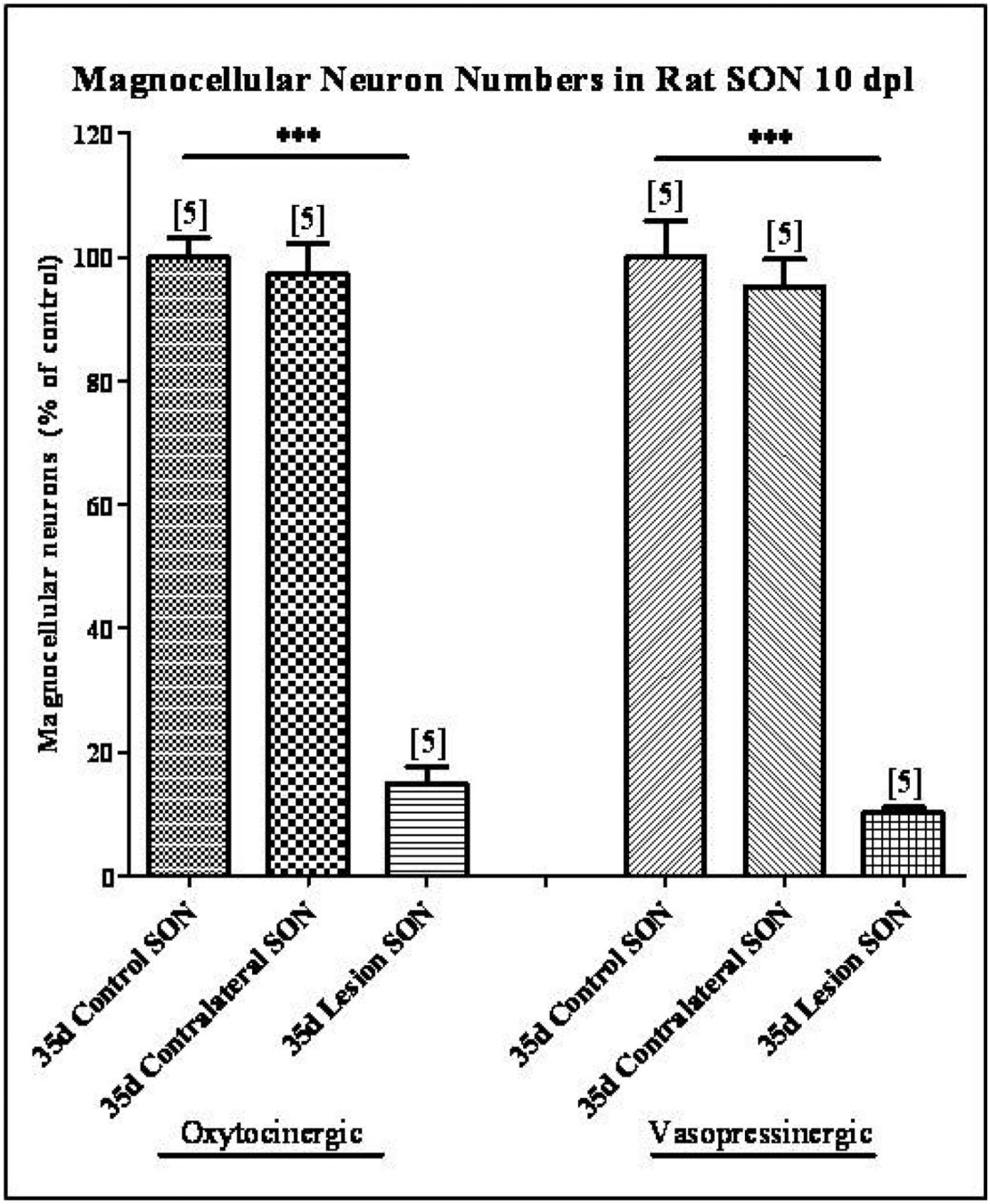

Fig. 2. Magnocellular neuron survival following unilateral lesion

Immunohistochemical labeling of OT and VP neurons was used to identify individual magnocellular neurons. Cell counts demonstrated no significant decrease in the number of OT or VP neurons in the SON contralateral to the unilateral lesion. However, at 10 dpl the numbers of OT and VP neurons were reduced by 85% and 90% respectively in the axotomized SON. Column bars and error bars represent the mean and SEM of each group. Each group is comprised of a minimum of six sections sampled from each of 5 animals. ***$p<0.0001$.

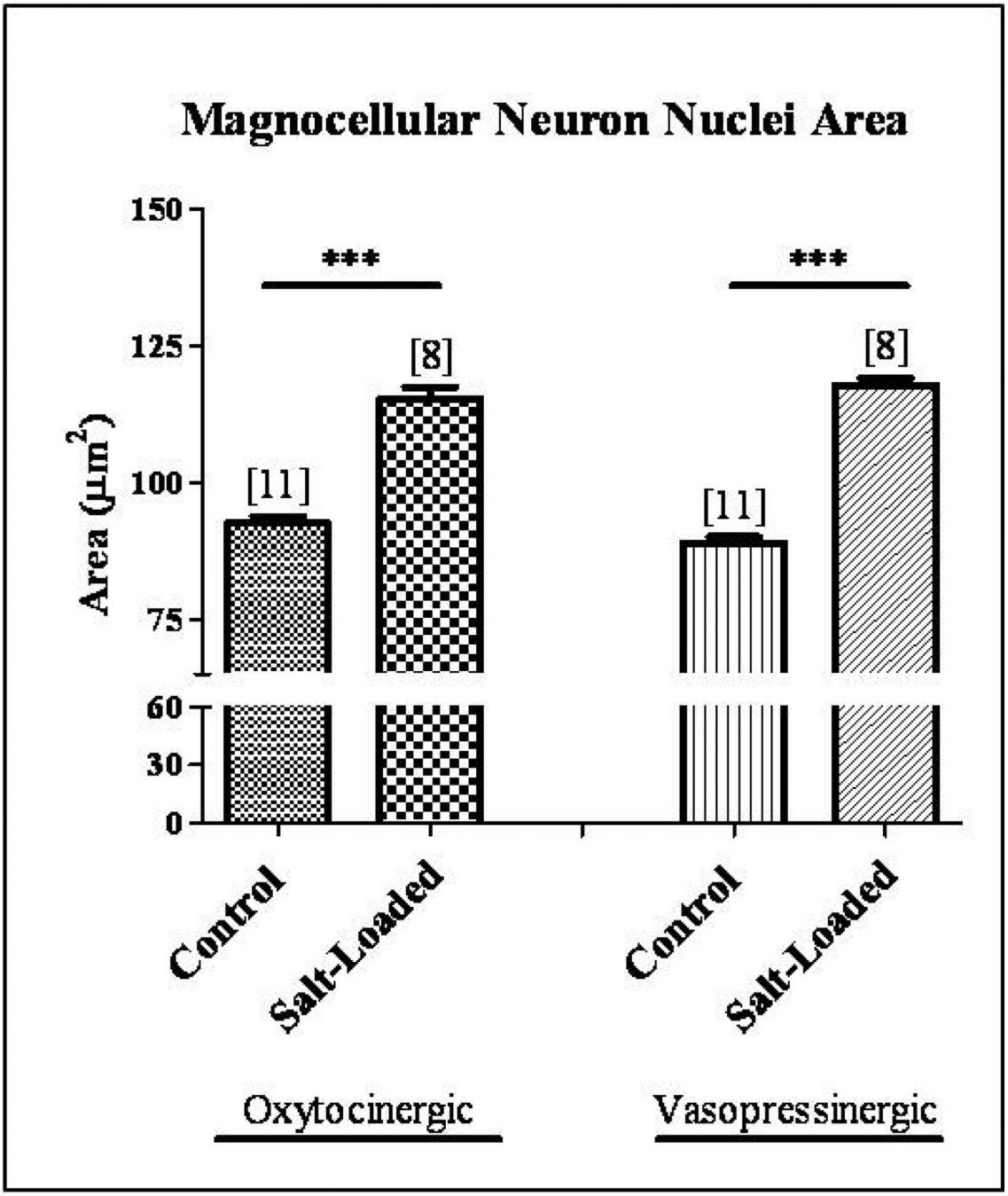

Fig. 3. Chronic salt-loading activates magnocellular neurons in the SON

Immunocytochemical analysis demonstrated a significant hypertrophy of 25% and 32% in OT and VP magnocellular neuron nuclei area, respectively, in the chronic salt-loaded SON. Column bars and error bars represent the mean and SEM of each group. ****p<0.0001*.

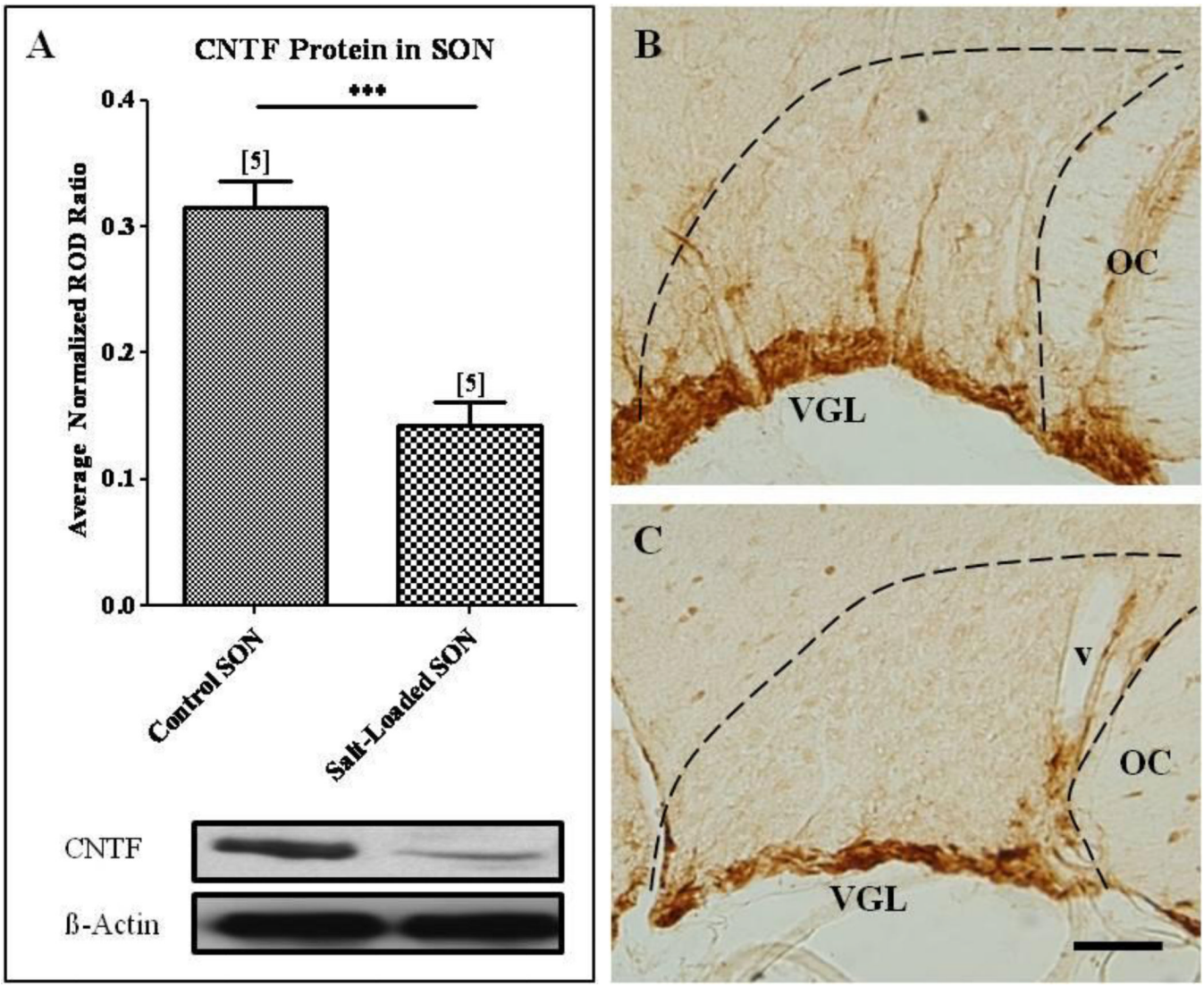

Fig. 4. Physiological activation of the SON decreased CNTF protein levels in the SON

(A) Western blot analysis revealed a significant decrease in CNTF protein levels in the salt-loaded SON compared to the age-matched control SON. Immunocytochemical analysis confirmed these results. A decrease in CNTF-immunoreactivity in the SON of the physiologically activated SON (C) was apparent when compared to the age-matched control SON (B). Column bars and error bars represent the mean and SEM of each group. OC, optic chiasm; v, blood vessel; VGL, ventral glial limitans. Scale bar = 100 μm. ***$p<0.0001$.

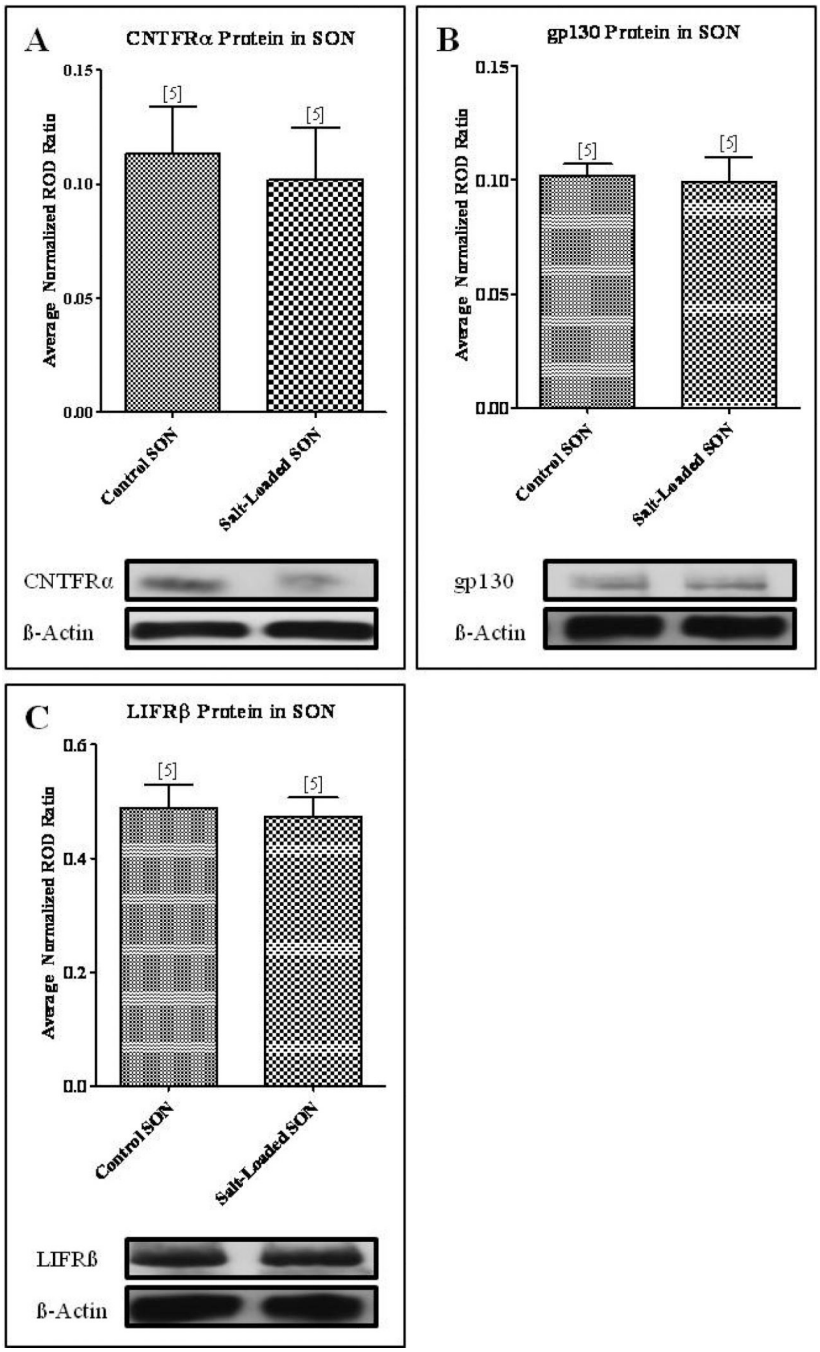

Fig. 5. Physiological activation of the SON resulted in no change in protein levels of the CNTF receptor components

Western blot analysis revealed no change in CNTFRα (A), gp130 (B), and LIFRβ (C) protein levels in the salt-loaded SON compared to the age-matched control SON. Column bars and error bars represent the mean and SEM of each group.

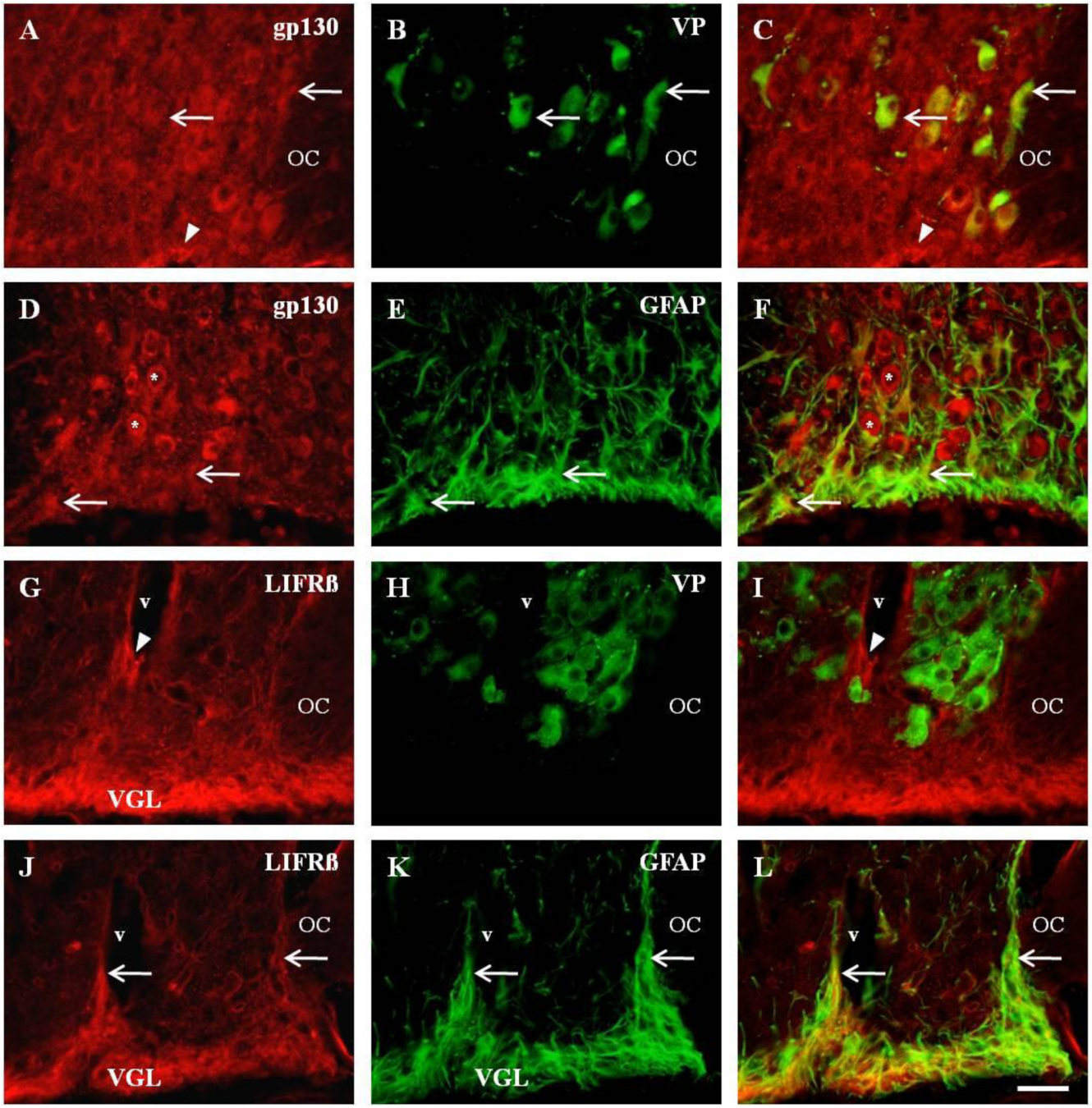

Fig. 6. Differential expression of CNTF receptor complex on astrocytes and magnocellular neurons

Dual fluorescent colocalization of anti-gp130 (A), with anti-VP (B), revealed colocalization in vasopressinergic neurons (C, arrows). Note the gp130-immunoreactive profiles in presumptive astrocytes in the ventral glial limitans (VGL) of the SON (A, C, arrowheads). Similar observations were observed with anti-OT (not shown). Immunocytochemical analysis also demonstrated colocalization of anti-gp130 (D), with GFAP-immunoreactive astrocytes (E), of the SON (F, arrows). Also present are presumptive magnocellular neurons that are immunopositive for gp130 (D, F, asterisks). Unlike gp130, there was no observable colocalization of anti-LIFRβ in the magnocellular neurons of the SON (G–I). Note the

LIFRβ-immunoreactive profiles surrounding blood vessels (v) in the SON (G, I, arrowheads) which do not colocalize with anti-VP (H) or anti-OT (not shown). However, strong LIFRβ-immunoreactivity in the ventral glial limitans (VGL) of the SON (J), revealed extensive colocalization of anti-LIFRβ (J), with anti-GFAP (K), throughout the entire SON (L, arrows). OC, optic chiasm; OT, oxytocin; v, blood vessel; VGL, ventral glial limitans; VP, vasopressin. Scale bar = 50 μm.